Received: December 19, 2024; **Accepted:** May 20, 2025; **Published:** May 20, 2025.
DOI. 10.30473/coam.2025.73126.1277
Winter-Spring (2025) Vol. 10, No. 1, (139-161)
Research Article

Open Access

Control and Optimization in Applied Mathematics - COAM

A Meshless Method for Optimal Control of Parabolic PDEs Using Rational Radial Basis Functions

Afrah Kadhim Saud Al-tameemi[1], **Mahmoud Mahmoudi**[1] ✉, **Majid Darehmiraki**[2]

[1]Department of Applied Mathematics, Faculty of Mathematical Sciences, University of Qom, Qom, Iran.
[2]Department of Mathematics, Behbahan Khatam Alanbia University of Technology, Khouzestan, Iran.

✉ **Correspondence:**
Mahmoud Mahmoudi
E-mail:
mahmoudi@qom.ac.ir

How to Cite
Al-tameemi, A.K.S., Mahmoudi, M., Darehmiraki, M. (2025). "A meshless method for optimal control of parabolic PDEs using rational radial basis functions", Control and Optimization in Applied Mathematics, 10(1): 139-161, doi: 10.30473/coam.2025.73126.1277.

Abstract. This study introduces an innovative approach for addressing optimal control problems related to parabolic partial differential equations (PDEs) through the application of rational radial basis functions (RBFs). Parabolic PDEs, which are instrumental in modeling time-dependent processes such as heat transfer and diffusion, pose significant computational challenges in optimal control due to the requirement for precise approximations of both state and adjoint equations. The proposed approach exploits the adaptability and spectral accuracy of rational RBFs within a meshless framework, effectively addressing the limitations of traditional discretization methods. By enhancing the accuracy and efficiency of control strategies, this method significantly contributes to advancing the theory and application of optimal control in dynamic systems. The tunable shape parameters of rational RBFs allow for accurate representation of solution characteristics, including steep gradients and localized behaviors. Additionally, their meshless framework adeptly accommodates complex geometries and boundary conditions, ensuring computational efficiency through the generation of sparse and well-conditioned system matrices. This paper also introduces a novel hybrid rational RBF, termed the Gaussian rational hybrid RBF. The efficacy of the proposed approach is validated through a series of benchmark tests and practical applications, highlighting its ability to achieve high accuracy with reduced computational effort. The findings illustrate the potential of rational RBFs as a robust and versatile tool for solving optimal control problems governed by parabolic PDEs, paving the way for further exploration of advanced rational RBF-based techniques in the field of computational optimal control.

Keywords. Meshless methods, Parabolic PDEs, Rational RBFs, Optimization, Gaussian rational hybrid RBF.

MSC. 49M41; 82M22.

1 Introduction

Optimal control problems involving partial differential equations (PDEs) are of significant interest to researchers in computational sciences due to their wide-ranging applications across various fields, including engineering, mathematics, finance, physics, and biology. Consequently, there has been extensive theoretical and quantitative research on this topic, particularly concerning the optimal control of elliptic PDEs. However, developing highly accurate mathematical frameworks for parabolic optimal control (POC) problems remains challenging due to the high dimensionality of discrete systems and the limitations of computational power. For comprehensive discussions on this topic, we direct readers to the works references in [2, 3, 31, 32, 35]. This study proposes an efficient numerical method to address the POC problems by utilizing rational radial basis functions (RBFs) [1] in conjunction with the Euler scheme.

The optimal control of parabolic PDEs is critical in various scientific and engineering domains, including heat transfer, diffusion-reaction systems, and financial modeling. However, solving these problems efficiently and accurately presents significant challenges due to their high dimensionality, the complexity of their solution space, and the necessity to satisfy both the state equation and the associated control constraints. Traditional numerical methods, such as the finite element and finite difference methods, often struggle to yield precise results without substantial computational resources. This issue is particularly pronounced when addressing problems characterized by steep gradients, localized features, or irregular geometries.

Let w denote the state variable and v the control variable. Consider $\Omega \subset \mathcal{R}^2$ to be a bounded polygonal domain with a Lipschitz boundary, and define $Q = \Omega \times (0, T]$. We formulate the POC problem as follows [11, 12, 13].

$$
\begin{aligned}
(POC:)\min \quad & J(w,v) = \tfrac{1}{2}\int_0^T \int_\Omega (w(.;\mu) - w_d)^2 d\Omega dt + \tfrac{\alpha}{2}\int_0^T \int_\Omega v^2(.;\mu) d\Omega dt \\
\text{s.t.} \quad & \\
& -\partial_t w + \mu L w = v, \quad \text{in } Q, \\
& w = 0, \quad \text{on } \Sigma, \\
& w(.,0) = 0, \quad \text{in } \Omega,
\end{aligned}
$$

where, L represents a spatial differential operator (e.g., the Laplacian) and $f(x,t)$ serves as a source term. It is crucial to establish appropriate boundary and initial conditions for the problem. The objective is to minimize the cost functional $J(w, \mathbf{v})$, where w is the state and $\mathbf{v}$ is the control vector, subject to the PDE constraint [22].

To approximate the solution $w(x,t)$, we employ rational RBFs. The general form of an RBF expansion can be expressed as follows:

$$
w(x,t) \approx \sum_{i=1}^{N} c_i \varphi(\|x - x_i\|),
$$

where φ denotes a radial basis function (e.g., Gaussian, inverse multiquadric), and c_i are the unknown coefficients to be determined [21, 37].

Previous research [20] has explored a space-time finite element approach with an iterative solution employing a semi-smooth Newton method, particularly addressing distributed tracking-type optimal control problems governed by the heat equation and state constraints. Additionally, the study by [36]

presented an efficient parallel splitting method utilizing linear finite elements for state and control variables, implementing the Crank-Nicolson scheme for temporal discretization, and a comprehensive Jacobian decomposition method with corrections to improve computational efficiency for parabolic PDE-constrained optimization problems. The analysis in [8] introduced a space-time finite element technique for addressing parabolic distributed optimal control problems by employing a coercive variational formulation and Lagrangian multipliers while adhering to Babuška-Brezzi criteria, leading to effective and reliable numerical approximations. Langer and Schafelner [18] examined locally stabilized space–time finite element techniques on entirely unstructured simplicial space–time meshes for the numerical resolution of the parabolic PDE-constrained optimization problems. Moreover, [9] examined the integral definition of the fractional Laplacian and analyzed a linear quadratic optimum control problem associated with the fractional heat equation, incorporating control constraints. For additional insights, we refer to [14, 17, 25, 26, 30].

Numerical methods, including the finite difference, finite element, and finite volume methods, are extensively utilized for solving PDEs [15]. However, these methods commonly rely on mesh-based formulations, necessitating grid generation that can be computationally expensive. Furthermore, their accuracy diminishes in non-smooth and non-regular domains, as the solution is typically evaluated only at discrete mesh points. To combat these issues, meshless techniques have been developed. In recent years, RBFs have emerged as a promising alternative in the numerical solution of PDEs, gaining popularity within the engineering and scientific communities due to their meshless nature and ease of extension to multi-dimensional problems. Meshless techniques utilize a collection of particles to effectively solve integral or partial differential equations under various boundary conditions, yielding accurate and stable solutions.

In the study conducted by [6], the authors introduced a rational RBF interpolation technique for estimating multivariate functions exhibiting poles or singularities in or near the approximation domain. This approach employed scattered point configurations, demonstrating flexibility concerning the problem's geometry. Shiralizadeh et al. [33] applied rational RBFs to solve the Allen-Cahn equation, particularly for problems characterized by steep fronts or sharp gradient solutions, utilizing rational RBFs to approximate spatial derivatives. Additionally, in [34], the authors employed the rational RBFs approach to address the Korteweg-de Vries equation, particularly in scenarios involving solutions with steep fronts or abrupt slopes. In reference [4], a local radial basis functions collocation method was introduced for solving the parabolic-parabolic Patlak-Keller–Segel model. The authors of [23] proposed a hybrid strategy combining meshless Galerkin and replicating kernel Hilbert space methods for quasi-linear parabolic equations. Furthermore, Zeng et al. [38] successfully resolved parabolic equations using a time-parareal coupled unsymmetric collocation meshless approach. Lastly, the paper [10] presented an efficient numerical method utilizing arbitrary collocation points for an economic growth model, employing RBF interpolation to approximate solutions for optimal control problems.

Motivation

Rational RBFs are recognized for their exceptional capability in solving PDEs across a wide range of frequency spectra. This characteristic renders them particularly effective for capturing the smoothness

and long-range interactions typical of parabolic PDEs. By employing rational RBFs, we can achieve accurate and efficient approximations for both the state and adjoint equations within the optimal control framework. The high accuracy of these approximations leads to faster convergence rates for optimization algorithms, while the compact support of certain rational RBFs enhances computational efficiency by producing sparse or well-conditioned system matrices. Moreover, the meshless nature of RBFs is ideal for numerous optimal control problems, as it allows for seamless integration of adaptive refinement and multi-resolution strategies.

In this context, the utilization of rational RBFs represents a promising approach to addressing the limitations inherent in traditional methods for optimal control. This flexibility and efficiency in numerically solving the space-time tracking the POC problem is particularly noteworthy, especially when employing standard L_2-regularization as a model problem. It is important to highlight that, to the best of our knowledge, this paper presents the first meshless method utilizing rational RBFs for optimal control problems governed by parabolic PDEs.

The structure of this study is organized as follows: Section 2 provides an overview of RBF interpolation and rational RBFs. Section 3 discusses the application of rational RBFs in solving the optimal control of parabolic PDEs. Section 4 presents numerical examples to demonstrate the effectiveness and correctness of the proposed method. Finally, Section 5 offers a concise conclusion.

2 Radial Basis Functions

This section introduces RBF interpolation and differentiation. A radial basis function is a real-valued function whose value is determined solely by the distance from a designated point y, termed the center, represented mathematically as $\psi(x, y) = \phi(\|x-y\|_2)$. RBFs may incorporate a free parameter ϵ, known as the shape parameter.

Consider a set of scattered node data defined as:

$$M = \{(x_i, g_i)|x_i \in \Omega,\ g_i \in \mathcal{R},\ for\, i = 1, \cdots, N\},$$

where $g : \Omega \to \mathbb{R}$ and $g(x_i) = g_i$. The RBF interpolant applied to the data from the scattered nodes is given by:

$$h(x) = \sum_{i=1}^{n} c_i \phi(\|x - x_i\|_2). \tag{1}$$

By enforcing $h(x_i) = g_i$, we can determine the unknown coefficients $\{c_i\}_{i=1}^n$. This leads to a linear system expressed as $\mathbf{Ac} = \mathbf{b}$, where $a_{ij} = \{\phi(x_i - x_j)\}_{i,j=1}^n$, and $b_i = f_i$ for $i = 1, \ldots, n$. The matrix $\mathbf{A}$ is commonly referred to as the RBF interpolation matrix or the RBF system matrix. For certain RBFs ϕ, this matrix remains consistently nonsingular. Notably, the completely monotonic multiquadratic RBF yields an invertible RBF system matrix, a property also shared by strictly positive definite RBFs such as inverse multiquadratics and Gaussians.

The following theorem establishes that, under specific conditions, the space of RBFs can approximate any continuous function arbitrarily precision [24, 28].

Theorem 1. Let $\phi : \mathbb{R}^d \to \mathbb{R}$ be a RBF (e.g., Gaussian, multiquadric, or inverse multiquadric), and let $\mathcal{F}$ be the space of all functions of the form:

$$f(x) = \sum_{i=1}^{N} w_i \phi(\|x - c_i\|),$$

where $w_i \in \mathbb{R}$, $c_i \in \mathbb{R}^d$ are centers, and $\|\cdot\|$ denotes the Euclidean norm.

Then, under mild conditions on ϕ (e.g., ϕ is continuous and not a polynomial), the space $\mathcal{F}$ is dense in the space of continuous functions $C(\mathbb{R}^d)$ with respect to the topology of uniform convergence on compact sets. Specifically, for any continuous function $g : \mathbb{R}^d \to \mathbb{R}$ and any compact set $K \subset \mathbb{R}^d$, and for any $\epsilon > 0$, there exists a function $f \in \mathcal{F}$ such that:

$$\sup_{x \in K} |f(x) - g(x)| < \epsilon.$$

This theorem is foundational to the theory of neural networks, interpolation, and approximation theory, as it justifies the application of RBFs for the approximation of continuous functions.

Rational RBFs represent a class of functions employed in various computational methods, including interpolation, approximation, and numerical solutions of PDEs. They combine the desirable features of traditional RBFs with a rational form, offering enhanced flexibility and regularization.

Common examples of standard RBFs include:

- Gaussian RBF: $\phi(r) = e^{-(\epsilon r)^2}$, where ϵ is the shape parameter.
- Multiquadric RBF: $\phi(r) = \sqrt{1 + (\epsilon r)^2}$,
- Inverse Multiquadric RBF: $\phi(r) = \frac{1}{\sqrt{1+(\epsilon r)^2}}$.

These RBFs are typically utilized for interpolation, surface fitting, and solving PDEs in a meshless manner.

A rational function is defined as the ratio of two polynomials. Rational RBFs are expressed as:

$$\phi_{rational}(r) = \frac{p(r)}{q(r)},$$

where $p(r)$ and $q(r)$ are polynomials, with $p(r)$ usually of lower degree than $q(r)$. This form of RBF offers several advantages, particularly in handling singularities or controlling decay behavior more flexibly compared to traditional RBFs.

One prevalent type of rational RBF is the rational quadratic function:

$$\phi_{\text{rq}}^{\epsilon,\alpha}(r) = \left(1 + \left(\frac{r}{\epsilon}\right)^2\right)^{-\alpha},$$

where r represents the radial distance $\|x - c\|$, ϵ is a shape parameter, and α is a positive real parameter that regulates the decay rate. This function consists of a constant polynomial in the numerator and a polynomial of degree 2 in the denominator. The rational quadratic RBF is smooth, and can effectively model both smooth and slightly irregular data compared to Gaussian RBFs.

Rational RBFs can engineered to exhibit faster decay at infinity, making them particularly useful for applications requiring the solution to diminish at large distances or to mitigate the bumpy behavior or

singularities inherent in some Gaussian RBFs when distances become large. The rational formulation facilitates better numerical properties, especially in cases where the data or solution may exhibit singular characteristics. Furthermore, rational RBFs are adept at managing behavior near domain boundaries or adapting to irregular data distributions.

In terms of regularization, rational RBFs often exhibit greater stability than standard RBFs, which enhances their robustness in specific numerical methods, especially for solving PDEs or inverse problems where smoothness and well-behaved solutions are essential. Overall, rational RBFs extend traditional radial basis functions by introducing a ratio of polynomials, offering improved flexibility, decay behavior control, and numerical stability. They are particularly advantageous in applications such as meshless methods for PDEs, surface fitting, and optimal control problems.

2.1 Gaussian Rational Hybrid RBF

The Gaussian Rational Hybrid RBF merges the smoothness characteristic of the Gaussian kernel with the localization flexibility inherent to rational functions. The proposed RBF is given by:

$$\phi_\beta^\sigma(r) = \frac{\exp\left(-\left(\frac{r}{\sigma}\right)^2\right)}{1+\beta r^2}.$$

The key features of the Gaussian Rational Hybrid RBF are highlighted as follows:

- Smoothness: The function derives its smoothness from the Gaussian kernel, which ensures a high degree of continuity.
- Flexibility: The inclusion of the rational term introduces a tunable parameter (β) that controls the tail behavior of the RBF, thereby enhancing its adaptability for various applications.
- Compact Support-Like Behavior: For large values of β, the RBF exhibits faster decay, resembling the properties of functions with compact support.

The derivative of the function with respect to r is expressed as:

$$\phi'(r) = \frac{-2r\exp\left(-\left(\frac{r}{\sigma}\right)^2\right)}{\sigma^2(1+\beta r^2)} - \frac{2\beta r\exp\left(-\left(\frac{r}{\sigma}\right)^2\right)}{(1+\beta r^2)^2}.$$

The related parameters are defined as below:

1. Shape Parameter (σ): This parameter dictates the spread of the Gaussian component, where smaller values yield sharper peaks.
2. Rational Parameter (β): This parameter modifies the tail behavior of the RBF, with larger values facilitating a more rapid decay and thereby localizing the influence of the function.

Theorem 2. The Gaussian Rational Hybrid RBF (GRH-RBF) defined as

$$\phi_\beta^\sigma(r) = \frac{\exp\left(-\left(\frac{r}{\sigma}\right)^2\right)}{1+\beta r^2}, \quad \sigma > 0, \beta \geq 0,$$

is strictly positive definite for any set of distinct nodes $\{x_i\}_{i=1}^N \subset \mathbb{R}^d$. Consequently, the interpolation matrix $\mathbf{A}$, defined by $A_{ij} = \phi_\beta^\sigma(\|x_i - x_j\|)$, is both positive definite and invertible.

Proof. A function $\phi : \mathbb{R}^d \to \mathbb{R}$ is classified as strictly positive definite if for any distinct points $\{x_i\}_{i=1}^N$, the quadratic form satisfies:

$$\sum_{i,j=1}^{N} c_i c_j \phi(\|x_i - x_j\|) > 0 \quad \forall \mathbf{c} \neq \mathbf{0}.$$

To analyze $\phi_\beta^\sigma(r)$, we rewrite it as a product:

$$\phi_\beta^\sigma(r) = \underbrace{\exp\left(-\left(\frac{r}{\sigma}\right)^2\right)}_{\text{Gaussian term } \phi_G(r)} \cdot \underbrace{\frac{1}{1+\beta r^2}}_{\text{Rational term } \phi_R(r)}.$$

The Gaussian $\phi_G(r) = e^{-(r/\sigma)^2}$ is known to be strictly positive definite, and its Fourier transform is another Gaussian, which is non-negative and integrable, thus adhering to Bochner's theorem. Consequently, the matrix $\mathbf{A}_G$ with entries $A_{G,ij} = \phi_G(\|x_i - x_j\|)$ is positive definite.

Additionally, the rational term $\phi_R(r) = (1 + \beta r^2)^{-1}$ is completely monotone. A function $\psi(r)$ is considered completely monotone if $(-1)^k \psi^{(k)}(r) \geq 0$ for all $k \geq 0$ and $r > 0$. For $\phi_R(r)$, the derivatives alternate in sign:

$$\phi_R'(r) = -\frac{2\beta r}{(1+\beta r^2)^2} \leq 0, \quad \phi_R''(r) \geq 0, \quad \text{etc.}$$

By the Bernstein-Widder theorem, $\phi_R(r)$ is the Laplace transform of a non-negative measure, ensuring its complete monotonicity. According to Schaback's theorem, if $\phi_G(r)$ is strictly positive definite and $\phi_R(r)$ is completely monotone with $\phi_R(0) > 0$, then their product $\phi_G(r)\phi_R(r)$ is strictly positive definite. In this case, $\phi_R(0) = 1 > 0$, and ϕ_G is strictly positive definite, which implies that $\phi_\beta^\sigma(r)$ inherits strict positive definiteness. The positive definiteness of $\mathbf{A}$ guarantees that $\mathbf{c}^T\mathbf{A}\mathbf{c} > 0$ for all $\mathbf{c} \neq \mathbf{0}$, ensuring that $\mathbf{A}$ is non-singular and thus provides a unique solution to the RBF interpolation problem. □

Theorem 3. For any function $f \in C^\infty([0,1])$, the GRH-RBF interpolant s_f satisfies the inequality:

$$\|f - s_f\|_{L^\infty} \leq Ce^{-c/\sqrt{h}},$$

where h denotes the fill distance, and $C, c > 0$ depend on σ, β, and f.

Proof. The analysis commences with the GRH-RBF given by

$$\phi(r) = \frac{e^{-(r/\sigma)^2}}{1+\beta r^2}.$$

The native space $\mathcal{N}_\phi$ employs the norm defined as:

$$\|f\|_\phi^2 = \sum_{k \in \mathbb{Z}} \frac{|\hat{f}(k)|^2}{\hat{\phi}(k)},$$

where $\hat{\phi}(k)$ denotes the Fourier transform of ϕ. The Fourier transform of ϕ exhibits dual decay behavior:

$$\hat{\phi}(k) \sim \begin{cases} e^{-\sigma^2 k^2/4} & \text{(Gaussian)}, \\ |k|^{-3} & \text{(Rational tail)}. \end{cases}$$

This hybrid decay ensures the exponential accuracy for smooth functions f and manages controlled conditioning through the rational term. By applying the sampling inequality:

$$\|f - s_f\|_{L^\infty} \leq P(h)\|f\|_\phi,$$

where the power function $P(h)$ is bounded by:

$$P(h) \leq \sup_k \left(1 - \frac{|\hat{\phi}(k)|}{\sum_j |\hat{\phi}(k - jh^{-1})|}\right).$$

For the GRH-RBF, we arrive at:

$$P(h) \leq C_1 e^{-c_1/h} + C_2 h^3.$$

As $h \to 0$, the exponential term predominates, resulting in:

$$\|f - s_f\|_{L^\infty} \leq C e^{-c/\sqrt{h}}.$$

The constants C and c depend on σ, β, properties of $\|f\|_{C^k}$, with higher derivatives of f further amplifying C. □

3 Methodology

The RBF interpolation of scattered data serves as the underlying framework for the meshless method that employs RBFs. The function $w(x)$ can be approximated using an RBF through a linear combination expressed as follows:

$$w(x) = \sum_{i=1}^{n} c_i \phi(r_i). \tag{2}$$

In this formulation, ϕ denotes the RBF, n represents the total count of data points, and c_i for $i = 1, \ldots, n$ are coefficients that need to be determined. It is noteworthy that most RBF-based methods are significantly influenced by the shape parameters associated with RBFs. The selection of the shape parameter is critical for ensuring the accuracy of the interpolation results, as various shape parameter values yield different RBF results within the same computational domain.

This section delineates the procedure for solving a POC problem. The approach begins with discretizing the time domain, followed by the spatial discretization utilizing rational radial basis functions. This approach facilitates a structured resolution of the state and adjoint equations based on the optimality conditions.

We consider the standard optimal control problem governed by a parabolic PDE as follows [19]

$$\min_{w,\, v} J(w, v) = \frac{1}{2} \int_0^T \int_\Omega (w(x,t) - w_d(x,t))^2 \, dx \, dt + \frac{\alpha}{2} \int_0^T \int_\Omega v(x,t)^2 \, dx \, dt,$$

subject to:

$$\frac{\partial w}{\partial t} - \Delta w = f(x,t) + v(x,t), \quad \text{in } \Omega \times (0,T],$$

with initial and boundary conditions:

$$w(x,0) = w^0(x), \quad w|_{\partial\Omega} = 0.$$

The first-order necessary optimality conditions are given by [16]:

1. State Equation:

$$\frac{\partial w}{\partial t} - \Delta w = f(x,t) + v(x,t), \tag{3}$$

2. Adjoint Equation:

$$-\frac{\partial p}{\partial t} - \Delta p = w - w_d, \quad p(x,T) = 0, \tag{4}$$

3. Control Update Rule:

$$v(x,t) = -\frac{1}{\alpha} p(x,t). \tag{5}$$

3.1 Time Discretization Using Finite Difference Method

To address the optimal control for parabolic PDEs using the rational RBF approach, we assume there are n_I inner points and n_B border nodes among the n total collection points within the domain, where $n = n_I + n_B$. Let $\Delta t = t_{i+1} - t_i$ denote the time step, with t^i representing the time value at stage i [5]. For all $t_i \leq t \leq t_{i+1}$, the POC problem is discretized using the following expression.

We discretize the time domain $[0,T]$ into N_t intervals, where the step size is given by $\Delta t = T/N_t$. The time steps are defined as $t^n = n\Delta t$ for $n = 0, 1, \ldots, N_t$.

1. State Equation (Forward Time Discretization): The state equation is discretized as follows:

$$\frac{w^{n+1}(x) - w^n(x)}{\Delta t} - \Delta w^{n+1}(x) = f^n(x) + v^n(x).$$

Rearranging this equation yields the update for $w^{n+1}(x)$:

$$w^{n+1}(x) = \Delta t \left(\Delta w^{n+1}(x) + f^n(x) + v^n(x)\right) + w^n(x). \tag{6}$$

2. Adjoint Equation (Backward Time Discretization): The adjoint equation is discretized as:

$$-\frac{p^{n+1}(x) - p^n(x)}{\Delta t} - \Delta p^n(x) = w^n(x) - w_d^n(x).$$

Rearranging this equation provides the update for $p^n(x)$:

$$p^n(x) = \Delta t \left(\Delta p^n(x) + w^n(x) - w_d^n(x)\right) + p^{n+1}(x). \tag{7}$$

3.2 Spatial Discretization Using Rational RBFs

For spatial discretization, we express both $w^n(x)$ and $p^n(x)$ in terms of rational RBFs as follows:

$$w^n(x) \approx \sum_{i=1}^{N} c_i^n \phi_i(x), \quad p^n(x) \approx \sum_{j=1}^{N} d_j^n \phi_j(x),$$

where $\phi_i(x)$ is the selected RBF with centers at x_i, and c_i^n and d_j^n are coefficients corresponding to time step n that require determination. By substituting these expansions into the time-discretized equations and applying Galerkin projection, we derive a system of algebraic equations for the coefficients c_i^n and d_j^n. The following outlines a comprehensive approach for implementing the RBF spectral technique in the optimal control of a PDE problem.

Algorithm 4 Optimal Control's Algorithm.

- Initialize $w^0(x)$, $v^0(x)$, and $p^{N_t}(x)$.
- Select an appropriate RBF, specify the RBF centers, determine the collocation sites, and establish a time step.
- Construct the required RBF interpolation and differentiation matrices outside of the primary time-stepping loop.

for $n = 0 : N_t - 1$ **do**

1. Solve for $w^{n+1}(x)$ using the state equation (6).
2. Solve for $p^n(x)$ utilizing the adjoint equation (7).
3. Update $v^n(x)$ according to the control update rule (5).

end for

- After completing the time-stepping, compute the error at the final time T to evaluate the accuracy.

This method ensures that the time-stepping procedure integrates seamlessly with the spatial discretization utilizing rational RBFs, resulting in efficient and accurate solutions.

3.3 Selection of Shape Parameter

The selection of the shape parameter ϵ in the RBF collocation methods plays a crucial role in determining both the accuracy and stability of the approximation. There is no global optimal shape parameter; rather,

its optimal value is influenced by factors such as the geometry of the problem, the spatial distribution of data points, and the desired trade-off between approximation accuracy and numerical stability [7].

Strategies for Selecting ϵ include the following:

1. Cross-Validation:
   - Conduct numerical experiments by solving the problem with different values of ϵ and evaluate the accuracy of the solutions using error metrics, such as L_2 and L_∞ norms.
   - Select the value of ϵ that yields the minimal error.
2. Domain-Based Rules of Thumb: A common rule is to set ϵ in relation to the average distance d between neighboring data points, such that:
$$\epsilon \sim \text{median}(d^2) \quad \text{or} \quad \epsilon \sim \frac{\max(d^2)}{k},$$
where k is a tuning constant (e.g., $k = 10$).
3. Adaptive Techniques: Implement an adaptive shape parameter that varies across the domain to more effectively capture local characteristics. This approach is particularly useful for problems characterized by highly non-uniform solutions.
4. Optimization: Optimize ϵ as a component of the solution process using numerical techniques, such as gradient descent or Bayesian optimization.

A general procedure for selecting ϵ includes the following steps:

- Begin with an initial estimate of $\epsilon \approx 0.5$ or $\epsilon \approx 1.0$.
- Gradually adjust ϵ, either increasing or decreasing it, and monitor its impact on accuracy and stability.

An improperly selected ϵ can lead to ill-conditioned system matrices during the interpolation or collocation process. Therefore, it is advisable to monitor the condition number of the matrices while adjusting ϵ. For time-dependent problems, it may be beneficial to adopt different ϵ values for various time steps or to adaptively adjust the parameter based on the behavior of the solution. The authors in [27] demonstrated the application of neural networks to determine optimal shape parameters for RBFs. They developed a multilayer perceptron using an unsupervised learning approach to predict shape parameters for inverse multiquadric and Gaussian kernels.

4 Numerical Examples

This section presents three numerical examples to illustrate the effectiveness of our proposed technique. The focus is on one-dimensional problems defined over the interval $\Omega = [0, 1]$. The optimality system defined by equations (3) and (4) yields accurate approximations for both the state and control functions.

The L_2 norm assesses the overall error across the entire domain, providing a holistic perspective on the method's accuracy, while the L_∞ norm highlights the maximum error at any single point, thereby demonstrating the method's efficacy in regions characterized by abrupt changes or fine details. All examples utilize the Gaussian rational hybrid RBF with a shape parameter of 0.5. The parameters for the optimal control problem for this section are established as follows:

$$\alpha = 10^{-6}, N = 32, \Delta t = 0.1, \beta = 1, \sigma = 1.$$

Example 1. For the POC problem, consider the exact solution for the state function given by:

$$w = t^2(1-t)^2(2-t)^2 \sin(\pi x).$$

The optimality system generates the control function u, the desired function w_d, and the initial condition w_0. Figure 1 illustrates the computational associated with the adjoint function and the state function for Example 1. The results obtained indicate that the solutions are quite accurate.

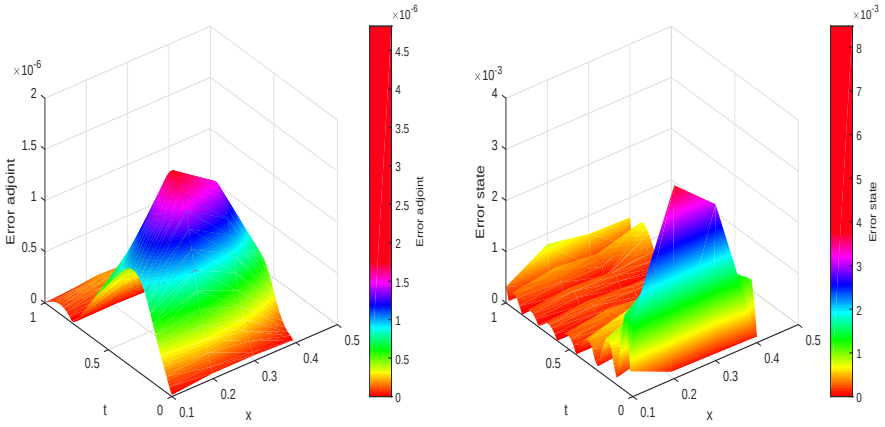

Figure 1: Approximation error of the adjoint and state functions in Example 1.

Figure 2 investigates the convergence of the proposed method applied to Example 1.

Figure 2 compares the exact and approximate state functions at various time steps in Example 1, demonstrating the accuracy of the proposed method using rational RBFs. The exact solution serves as a benchmark against which the performance of the method can be evaluated in capturing the dynamics of the state function over time. The figure reflects an excellent correspondence between the exact and approximated solutions throughout all time intervals. This comparison reinforces the robustness of the rational RBF method in solving time-dependent parabolic PDEs. The results confirm that the method not only retains the essential physical features of the solution but also achieves high accuracy consistently during the time evolution.

Table 1 provides the L_2 and L_∞ norm errors for the calculated computed state and adjoint functions at different time points in Example 1. The results presented in the table highlights the high degree of accuracy attained by the rational RBF method across all time steps. The errors remain consistently small, underscoring the method's robustness in solving the state and adjoint equations. Notably, the L_∞ errors

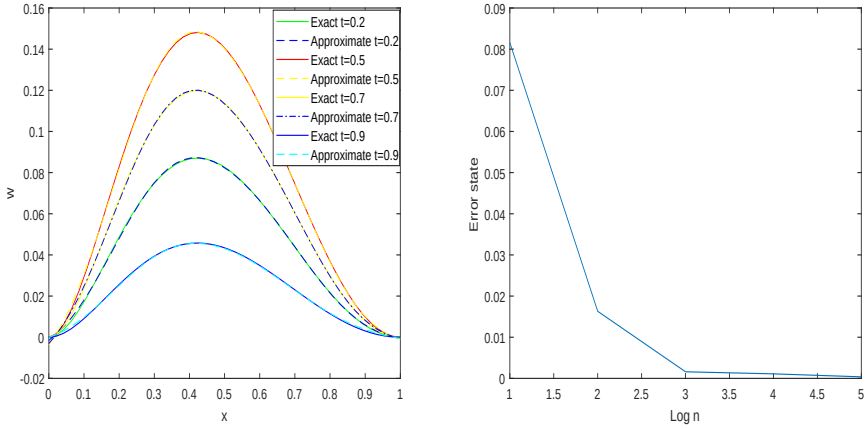

Figure 2: Comparisons of analytical and approximate solutions of $w(x,t)$ at $t = 0.2$s, $t = 0.5$s, $t = 0.7$s and $t - 0.9$s (left) and the error plot as a function of N (right) in Example 1.

Table 1: Values of L_2 and L_∞ errors for the state and adjoint functions at various time points in Example 1

Error	$t = 0.2$	$t = 0.5$	$t = 0.7$	$t = 0.9$
$\|w - \bar{w}\|_{L_2}$	0.0072-E3	0.0146-E3	0.0128-E3	0.1477-E3
$\|w - \bar{w}\|_{L_\infty}$	0.0018	0.0031	0.0025	0.0010
$\|v - \bar{v}\|_{L_2}$	0.5549-E6	0.8523-E6	0.6547-E6	0.2178-E6
$\|v - \bar{v}\|_{L_\infty}$	0.0806-E5	0.1301-E5	0.1024-E5	0.0357-E5

are well-controlled, indicating the ability of the rational RBFs to effectively manage steep gradients and localized variations.

The table illustrates that the error patterns conform to expectations based on the properties of rational RBFs, such as their accuracy and adeptness in handling complex solution landscapes. The gradual variation of errors over time further emphasizes the stability of the method when applied to time-dependent parabolic PDEs. These results affirm that the proposed approach is not only precise but also computationally efficient, rendering it a viable option for addressing optimal control problems constrained by parabolic PDEs. Additionally, in Table 2, the coefficients utilized in the approximation of the state function are detailed.

Example 2. Consider the exact solution for the state function in this POC problem defined as follows:

$$w = t^3(1-t)^3 \sin(\pi x).$$

In this example, we will similarly analyze the performance of the proposed method, focusing on the accuracy of the approximated state and control functions against the exact solutions. The optimality system yields the control function u, the desired function w_d, and the initial condition w_0. Figure 3 illustrates the computational error with both the adjoint and the state functions for Example 2. The results indicate a high level of accuracy.

Table 2: Values of coefficients c_i for $i = 1, 5, 10, 15$ used to approximate the state function at various values time points in Example 1

Coefficient	$t = 0.2$	$t = 0.5$	$t = 0.7$	$t = 0.9$
c_1	-0.1367	-0.2170	-0.1756	-0.0561
c_5	0.1411	0.2233	0.1807	0.1120
c_{10}	0.1661	0.2541	0.2056	0.0997
c_{15}	0.0244	0.0381	0.0308	0.0104

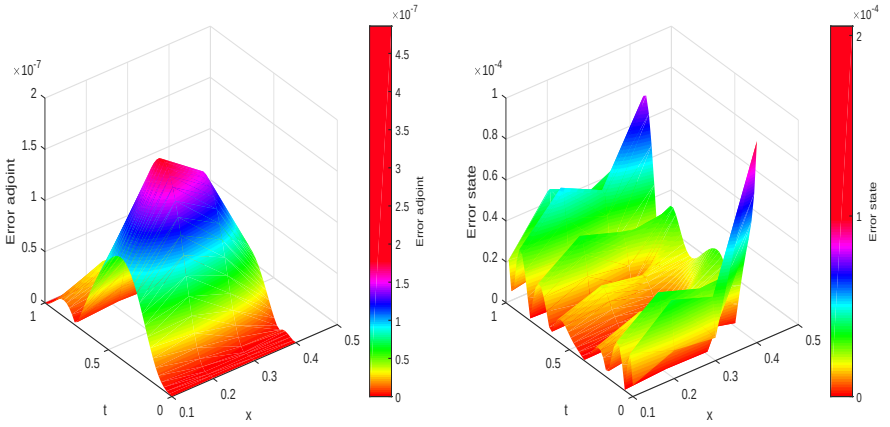

Figure 3: Approximation error of the adjoint and state functions in Example 2.

In Figure 4, we examine the convergence of the proposed method as applied to Example 2.

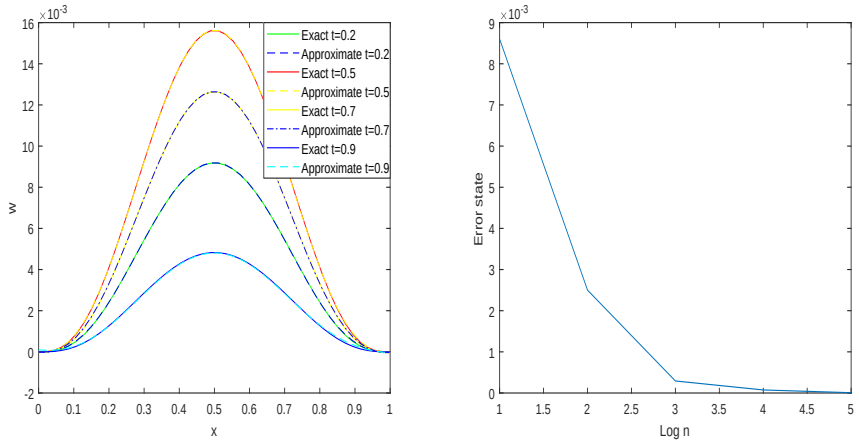

Figure 4: Comparison of analytical and approximate solutions of $w(x, t)$ at $t = 0.2$s, $t = 0.5$s, $t = 0.7$s and $t - 0.9$s (left), the error plot as a function of N (right) in Example 2.

Figure 4 presents a comparison of the exact and estimated state functions from Example 2 across various time instances, demonstrating the accuracy of the proposed method utilizing rational RBFs. The exact solution, positioned alongside the approximated solution, serves as a benchmark for evaluating the method's performance in accurately capturing the dynamics of the state function over time. The figure exhibits a remarkable alignment between the exact and approximated solutions throughout all time intervals.

Table 3: Values of L_2 and L_∞ norm errors for state and control functions at various time points in Example 2

Error	$t = 0.2$	$t = 0.5$	$t = 0.7$	$t = 0.9$
$\|w - \bar{w}\|_{L_2}$	0.0120-E4	0.0181-E4	0.0137-E4	0.1372-E4
$\|w - \bar{w}\|_{L_\infty}$	0.0642-E3	0.1093-E3	0.0884-E3	0.0835-E3
$\|v - \bar{v}\|_{L_2}$	0.561-E7	0.8888-E7	0.6928-E7	0.2445-E7
$\|v - \bar{v}\|_{L_\infty}$	0.0851-E6	0.1353-E6	0.1054-E6	0.0354-E6

Table 3 reports the L_2 and L_∞ norm errors for the computed state and control functions at various time points in Example 2. The results displayed in the table highlight the high accuracy degree of accuracy achieved by the rational RBF method across all time steps. The errors remain consistently low, reinforcing the robustness of the method in solving the state and control equations. Notably, the L_∞ errors are well-controlled, indicating the capability of the rational RBFs to effectively manage steep gradients and localized variations. Additionally, Table 4, presents the coefficients utilized in the approximation of the state function.

Table 4: Values of coefficients c_i, $i = 1,\ 5,\ 10,\ 15$ used to approximate the state function at various values time points in Example 2

Coefficient	$t = 0.2$	$t = 0.5$	$t = 0.7$	$t = 0.9$
c_1	-0.0078	-0.0130	-0.0105	-0.0030
c_5	0.0134	0.0227	0.0184	0.0112
c_{10}	0.0120	0.0202	0.0164	0.0083
c_{15}	0.0053	0.0089	0.0072	0.0026

In Table 5, we compare the performance of the multi-quadratic RBF method, as highlighted in [29] with that of rational RBF method.

The comparison in Table 5 illustrates the performance differences between the multi-quadratic and rational RBF methods, emphasizing the advantages of the latter in terms of accuracy and reliability across the evaluated time points. Through this analysis, it is evident that the rational RBF method provides superior performance in solving the POC problem, successfully capturing the underlying solution dynamics while maintaining computational efficiency and accuracy.

Example 3. Consider the exact solution for the state function in the context of the POC problem, expressed as:

Table 5: Comparison between multi-quadratic RBF method and the rational RBF method in Example 2

Error	$t = 0.2$	$t = 0.5$	$t = 0.7$	$t = 0.9$
$\|w - \bar{w}\|_{L_2}(MQ)$	0.1115-E3	0.0379-E3	0.0309-E3	0.0121-E3
$\|w - \bar{w}\|_{L_2}(Rational)$	0.1213-E4	0.0181-E4	0.0137-E4	0.1372-E4
$\|v - \bar{v}\|_{L_2}(MQ)$	0.1172-E6	0.3681-E6	0.3706-E6	0.2329-E6
$\|v - \bar{v}\|_{L_2}(Rational)$	0.5662-E7	0.8888-E7	0.6928-E7	0.2445-E7

$$w = t^2(1-t)^2x^4(1-x)^5.$$

The optimality system generates the control function u, the desired function w_d, and the initial condition w_0. Figure 5 illustrates the computational errors associated with both the adjoint and the state functions for Example 3. The results presented indicate a high level of accuracy in the solutions.

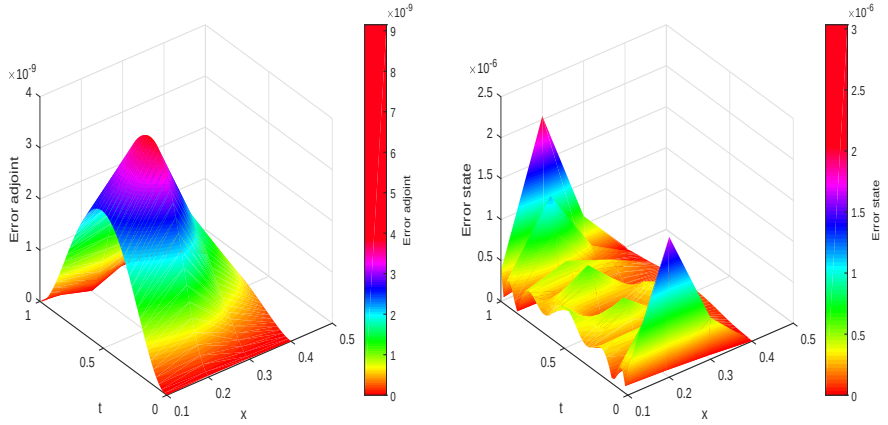

Figure 5: Approximation error of the adjoint and state functions in Example 3.

In Figure 6, the convergence behavior of the proposed method applied in Example 3 is examined.

Figure 6 presents a comparison of the exact and approximated state functions for various time instances in Example 3, showcasing at different times, the effectiveness of the proposed rational RBFs. The exact solution is depicted alongside the approximated solution to serve as a benchmark for evaluating the method's performance in accurately capturing the dynamics of the state function over time. The figure illustrates excellent correspondence between the exact and approximated solutions across all time intervals.

Table 6 provides the L_2 and L_∞ norm errors for the computed state and adjoint functions at various time points in Example 3. The results in the table indicate a high degree of accuracy achieved by the rational RBF method across all time steps. The errors remain consistently low, highlighting the robustness in solving both the state and adjoint equations. Importantly, the L_∞ errors are well-controlled, demonstrating the rational RBFs' efficacy in effectively managing steep gradients and localized variations. The results affirm that the proposed approach not only retains essential solution characteristics

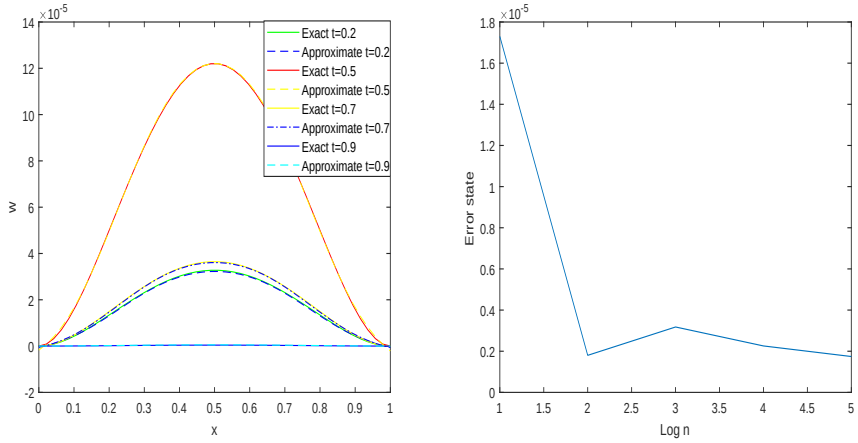

Figure 6: Comparisons of analytical and approximate solutions of $w(x,t)$ at $t = 0.2$s, $t = 0.5$s, $t = 0.7$s and $t = 0.9$s (left), along with the error plot as a function of N (right) in Example 3.

Table 6: Values of RMS and L_∞ errors for the state and control functions at various time points in Example 3

Error	$t = 0.2$	$t = 0.5$	$t = 0.7$	$t = 0.9$
$\|w - \bar{w}\|_{L_2}$	0.1879-E5	0.1194-E5	0.1289-E5	0.0554-E5
$\|w - \bar{w}\|_{L_\infty}$	0.0492-E5	0.1859-E5	0.0550-E5	0.0123-E5
$\|v - \bar{v}\|_{L_2}$	0.2070-E8	0.2676-E8	0.1780-E8	0.0497-E8
$\|v - \bar{v}\|_{L_\infty}$	0.2680-E8	0.3481-E8	0.2294-E8	0.0642-E8

but also maintains high accuracy throughout the temporal domain, thereby validating its applicability in optimal control problems governed by parabolic partial differential equations.

Example 4. Consider the exact solution for the state function in the context of the POC problem, defined as follows:

$$w = (t^{\sqrt{2}} + t^{2.5})x^3.$$

The optimality system generates the control function u, the desired function w_d, and the initial condition w_0. Figure 7 illustrates the computational errors associated with both the adjoint and the state functions for Example 4. The results indicate a high degree of accuracy in the approximations.

In Figure 8, we examine the convergence behavior of the proposed method for Example 4.

Figure 8 offers a comparison between the exact and approximated state functions for various time points in Example 4, at demonstrating the accuracy of the proposed method utilizing rational RBFs. The exact solution, presented alongside the approximated solution, serves as a benchmark for evaluating the method's performance in capturing the dynamics of the state function over time. The figure illustrates excellent agreement between the exact and approximated solutions across considered all time intervals.

Table 7 summarizes the L_2 and L_∞ norm errors for the computed state and adjoint functions at various time points in Example 4. The results presented in the table demonstrate the high accuracy achieved

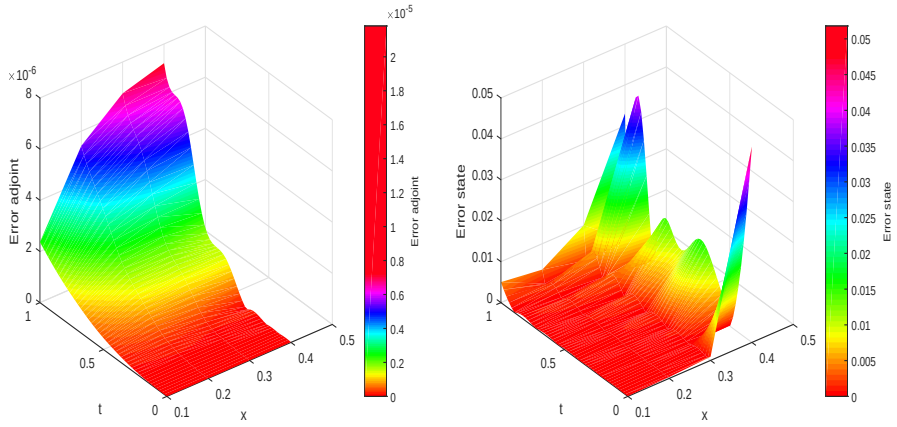

Figure 7: Approximation errors of the adjoint and state functions in Example 4.

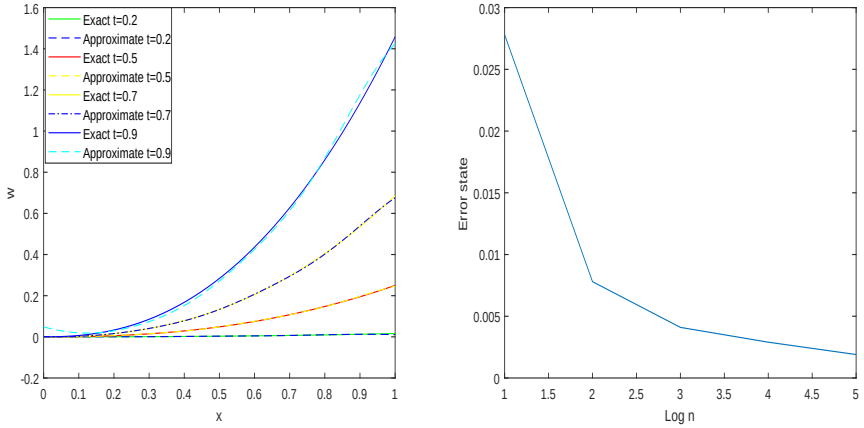

Figure 8: Comparison of analytical and approximate solutions of $w(x,t)$ at $t = 0.2$s, $t = 0.5$s, $t = 0.7$s and $t = 0.9$s (left), along with error plots based on values of N (right) in Example 4.

Table 7: Values of RMS and L_∞ errors for state and control functions at various time points in Example 4

Error	$t = 0.2$	$t = 0.5$	$t = 0.7$	$t = 0.9$
$\|w - \bar{w}\|_{L_2}$	0.0019	0.1194	0.1289	0.0109
$\|w - \bar{w}\|_{L_\infty}$	0.1229-E5	0.2828-E5	0.3565-E5	0.3918-E5
$\|v - \bar{v}\|_{L_2}$	0.0050	0.0037	0.0101	0.0478
$\|v - \bar{v}\|_{L_\infty}$	0.2364-E5	0.5427-E5	0.6773-E5	0.7250-E5

by the rational RBF method across all time steps. The errors are consistently low, underscoring the method's robustness in solving the state and adjoint equations. Furthermore, the L_∞ errors are effec-

tively well-controlled, indicating the rational RBFs' capability to manage steep gradients and localized variations adeptly.

This example demonstrates the effectiveness of the proposed method in accurately solving the POC problem, achieving high precision in both state and adjoint functions over various time intervals. The results highlight the robustness of the rational RBF approach and its applicability in addressing complex dynamic systems.

5 Conclusion

This paper introduces a meshless approach utilizing rational radial basis functions (RBFs) to address the optimal control problem associated with parabolic partial differential equations (PDEs). By using the precise and adaptable characteristics of rational RBFs, the proposed method effectively navigates the computational challenges inherent in these complex, dynamic problems. Furthermore, we have developed a hybrid rational RBF interpolation technique for diverse applications. This hybrid approach capitalizes on the strengths of both Gaussian and quadratic RBFs, allowing for enhanced flexibility and accuracy depending on the specific nature of the problem. The numerical results demonstrate the robustness and efficacy of the proposed method, with the estimated state and adjoint functions closely approximating the exact solutions. The observed small L_2 and L_∞ errors across various time points, coupled with the method's ability to handle sharp transitions and intricate solution features, indicate its potential as a reliable tool for solving parabolic PDEs in optimal control scenarios. Notably, the meshless nature of the rational RBF approach facilitates the management of complex geometries and boundary conditions while ensuring computational efficiency. These attributes make the method especially advantageous in applications where traditional grid-based techniques may falter or prove or computationally prohibitive. In summary, the proposed rational RBF framework presents a powerful, precise, and flexible methodology for solving optimal control problems involving parabolic PDEs. Future research could expand this approach encompass to more complex systems, such as nonlinear PDEs or multiphysics problems, while also exploring the integration of adaptive strategies to further enhance efficiency and scalability.

Declarations

Availability of Supporting Data

All data generated or analyzed during this study are included in this published paper.

Funding

The authors conducted this research without any funding, grants, or support.

Competing Interests

The authors declare that they have no competing interests relevant to the content of this paper.

Authors' Contributions

The main text of manuscript is collectively written by the authors.

References

[1] Buhmann, M.D., De Marchi, S., Perracchione, E. (2020). "Analysis of a new class of rational RBF expansions", *IMA Journal of Numerical Analysis*, 40(3), 1972-1993, doi:10.1093/imanum/drz015.

[2] Darehmiraki, M., Rakhshan, S.A. (2023). "Radial basis functions for the zero sum differential game with fractional derivatives", *International Journal of Applied and Computational Mathematics*, 9(5), 90, doi:10.1007/s40819-023-01587-3.

[3] Darehmiraki, M., Rezazadeh, A., Ahmadian, A., Salahshour, S. (2022). "An interpolation method for the optimal control problem governed by the elliptic convection–diffusion equation", *Numerical Methods for Partial Differential Equations*, 38(2), 137-159, doi:10.1002/num.22625.

[4] Dehghan, M., Abbaszadeh, M., Mohebbi, A. (2015). "A meshless technique based on the local radial basis functions collocation method for solving parabolic–parabolic Patlak–Keller–Segel chemotaxis model", *Engineering Analysis with Boundary Elements*, 56, 129-144, doi:10.1016/j.enganabound.2015.02.005.

[5] Fabien, M.S. (2014). "A radial basis function (RBF) method for the fully nonlinear 1D Serre Green-Naghdi equations", *arXiv preprint arXiv:1407.4300*, doi:10.48550/arXiv.1407.4300.

[6] Farazandeh, E., Mirzaei, D. (2021). "A rational RBF interpolation with conditionally positive definite kernels", *Advances in Computational Mathematics*, 47, 1-21, doi:10.1007/s10444-021-09900-8.

[7] Fasshauer, G.E., Zhang, J.G. (2007). "On choosing optimal shape parameters for RBF approximation", *Numerical Algorithms*, 45, 345-368, doi:10.1007/s11075-007-9072-8.

[8] Fuhrer, T., Karkulik, M. (2022). "Space-time finite element methods for parabolic distributed optimal control problems", *arXiv preprint arXiv:2208.09879*, doi:10.48550/arXiv.2208.09879.

[9] Glusa, C., Otarola, E. (2021). "Error estimates for the optimal control of a parabolic fractional PDE", *SIAM Journal on Numerical Analysis*, 59(2), 1140-1165, doi:10.1137/19M1267581.

[10] Golbabai, A., Safaei, N., Molavi-Arabshahi, M. (2022). "Numerical solution of optimal control problem for economic growth model using RBF collocation method", *Computational Methods for Differential Equations*, 10(2), 327-337, doi:10.22034/cmde.2021.40223.1757.

[11] Gotschel, Minion, M.L. (2019). "An efficient parallel-in-time method for optimization with parabolic PDEs", *SIAM Journal on Scientific Computing*, 41(6), C603-C626, doi:10.1137/19M1239313.

[12] Grubisic, L., Lazar, M., Nakic, I., Tautenhahn, M. (2023). "Optimal control of parabolic equations–a spectral calculus based approach", *SIAM Journal on Control and Optimization*, 61(5), 2802-2825, doi:10.1137/21M1449762.

[13] Guth, P.A., Kaarnioja, V., Kuo, F.Y., Schillings, C., Sloan, I.H. (2024). "Parabolic PDE-constrained optimal control under uncertainty with entropic risk measure using quasi-Monte Carlo integration", *Numerische Mathematik*, 156(2), 565-608, doi:10.1007/s00211-024-01397-9.

[14] Hashemi Borzabadi, A., Gholami Baladezaei, M., Ghachpazan, M. (2024). "A sub-ordinary approach to achieve near-exact solutions for a class of optimal control problems", *Control and Optimization in Applied Mathematics*, 9(2), 1-19, doi:10.30473/coam.2024.70834.1254.

[15] Heidari, M., Ghovatmand, M., Skandari, M.N., Baleanu, D. (2023). "Numerical solution of reaction–diffusion equations with convergence analysis", *Journal of Nonlinear Mathematical Physics*, 30(2), 384-399, doi:10.1007/s44198-022-00086-1.

[16] Herzog, R., Kunisch, K. (2010). "Algorithms for PDE□constrained optimization", *GAMM□Mitteilungen*, 33(2), doi:10.1002/gamm.201010013.

[17] Huang, Y., Mohammadi Zadeh, F., Hadi Noori Skandari, M., Ahsani Tehrani, H., Tohidi, E. (2021). "Space–time Chebyshev spectral collocation method for nonlinear time□fractional Burgers equations based on efficient basis functions", *Mathematical Methods in the Applied Sciences*, 44(5), 4117-4136, doi:10.1002/mma.7015.

[18] Langer, U., Schafelner, A. (2022). "Adaptive space–time finite element methods for parabolic optimal control problems", *Journal of Numerical Mathematics*, 30(4), 247-266, doi:10.1515/jnma-2021-0059.

[19] Langer, U., Steinbach, O., Yang, H. (2024). "Robust space-time finite element methods for parabolic distributed optimal control problems with energy regularization", *Advances in Computational Mathematics*, 50(2), 1-30, doi:10.1007/s10444-024-10123-w.

[20] Loscher, R., Reichelt, M., Steinbach, O. (2024). "Efficient solution of state-constrained distributed parabolic optimal control problems", *arXiv preprint arXiv:2410.06021*, doi:10.48550/arXiv.2410.06021.

[21] Luo, D., O'Leary-Roseberry, T., Chen, P., Ghattas, O. (2023). "Efficient PDE-constrained optimization under high-dimensional uncertainty using derivative-informed neural operators", *arXiv preprint arXiv:2305.20053*, doi:10.48550/arXiv.2305.20053.

[22] Mahmoudi, M., Shojaeizadeh, T., Darehmiraki, M. (2021). "Optimal control of time-fractional convection–diffusion–reaction problem employing compact integrated RBF method", *Mathematical Sciences*, 1-14, doi:10.1007/s40096-021-00434-0.

[23] Mesrizadeh, M., Shanazari, K. (2021). "Meshless Galerkin method based on RBFs and reproducing Kernel for quasi-linear parabolic equations with Dirichlet boundary conditions", *Mathematical Modelling and Analysis*, 26(2), 318-336, doi:10.3846/mma.2021.11436.

[24] Micchelli, C.A. (1986). "Interpolation of scattered data: Distance matrices and conditionally positive definite functions", *Constructive Approximation*, 2(1), 11-22, doi:10.1007/978-94-009-6466-2-7.

[25] Mohammadizadeh, F., Tehrani, H. A., Noori Skandari, M.H. (2019). "Chebyshev pseudo-spectral method for optimal control problem of Burgers' equation", *Iranian Journal of Numerical Analysis and Optimization*, 9(2), 77-102, doi:10.22067/ijnao.v9i2.72109.

[26] Mohammadizadeh, F., Tehrani, H.A., Georgiev, S.G., Noori Skandari, M.H. (2020). "An optimal control problem associated to a class of fractional Burgers' equations", *Asian-European Journal of Mathematics*, 13(04), 2050079, doi:10.1142/S1793557120500795.

[27] Mojarrad, F.N., Veiga, M.H., Hesthaven, J.S., Offner, P. (2023). "A new variable shape parameter strategy for RBF approximation using neural networks", *Computers and Mathematics with Applications*, 143, 151-168, doi:10.1016/j.camwa.2023.05.005.

[28] Park, J., Sandberg, I.W. (1991). "Universal approximation using radial-basis-function networks", *Neural Computation*, 3(2), 246-257, doi:10.1162/neco.1991.3.2.246.

[29] Pearson, J.W., Wathen, A.J. (2013). "Fast iterative solvers for convection-diffusion control problems", *Electronic Transactions on Numerical Analysis*, 40, 294-311.

[30] Peykrayegan, N., Ghovatmand, M., Noori Skandari, M.H., Shateyi, S. (2024). "Numerical solution of nonlinear fractional delay integro-differential equations with convergence analysis", *Indian Journal of Pure and Applied Mathematics*, 1-21, doi:10.1007/s13226-024-00620-5.

[31] Rezazadeh, A., Darehmiraki, M. (2024). "A fast Galerkin-spectral method based on discrete Legendre polynomials for solving parabolic differential equation", *Computational and Applied Mathematics*, 43(6), 315, doi:10.1007/s40314-024-02792-6.

[32] Rezazadeh, A., Mahmoudi, M., Darehmiraki, M. (2020). "A solution for fractional PDE constrained optimization problems using reduced basis method", *Computational and Applied Mathematics*, 39(2), 1-17, doi:10.1007/s40314-020-1092-1.

[33] Shiralizadeh, M., Alipanah, A., Mohammadi, M. (2023). "Approximate solutions to the Allen–Cahn equation using rational radial basis functions method", *Iranian Journal of Numerical Analysis and Optimization*, 13(2), 187-204, doi:10.22067/ijnao.2022.76010.1123.

[34] Shiralizadeh, M., Alipanah, A., Mohammadi, M. (2023). "A numerical method for KdV equation using rational radial basis functions", *Computational Methods for Differential Equations*, 11(2), 303-318, doi:10.22034/cmde.2022.51967.2171.

[35] Shojaeizadeh, T., Mahmoudi, M., Darehmiraki, M. (2021). "Optimal control problem of advection-diffusion-reaction equation of kind fractal-fractional applying shifted Jacobi polynomials", *Chaos, Solitons and Fractals*, 143, 110568, doi:10.1016/j.chaos.2020.110568.

[36] Song, H., Zhang, J., Hao, Y. (2023). "A splitting algorithm for constrained optimization problems with parabolic equations", *Computational and Applied Mathematics*, 42(205), doi:10.1007/s40314-023-02343-5.

[37] Su, L. (2019). "A radial basis function (RBF)-finite difference (FD) method for the backward heat conduction problem", *Applied Mathematics and Computation*, 354, 232-247, doi:10.1016/j.amc.2019.02.035.

[38] Zeng, Y., Duan, Y., Liu, B.S. (2021). "Solving 2D parabolic equations by using time parareal coupling with meshless collocation RBFs methods", *Engineering Analysis with Boundary Elements*, 127, 102-112, doi:10.1016/j.enganabound.2021.03.008.